Proapoptotic N-truncated BCL-xL protein activates endogenous mitochondrial channels in living synaptic terminals

Elizabeth A. Jonas*†, John A. Hickman‡, Mushtaque Chachar*, Brian M. Polster§, Teresa A. Brandt§, Yihru Fannjiang¶, Iva Ivanovska¶, Gorka Basañez‖, Kathleen W. Kinnally, Joshua Zimmerberg†‖, J. Marie Hardwick§¶††, and Leonard K. Kaczmarek†,†††‡‡**

Departments of ‡‡Pharmacology and *Internal Medicine, Yale University School of Medicine, 333 Cedar Street, New Haven, CT 06520; ‡Institut de Recherches Servier, 125 Chemin de Ronde, 78290 Croissy sur Seine, France; §Department of Molecular Microbiology and Immunology, Johns Hopkins University School of Public Health, 615 North Wolfe Street, Baltimore, MD 21205; ¶Department of Pharmacology and Molecular Sciences, Johns Hopkins University School of Medicine, 725 North Wolfe Street, Baltimore, MD 21205; ‖Laboratory of Cellular and Molecular Biophysics, National Institute of Child Health and Development, National Institutes of Health, 10 Center Drive, Bethesda, MD 20892; **Department of Basic Sciences, New York University College of Dentistry, New York, NY 10010; and †Marine Biological Laboratory, Woods Hole, MA 02543

Edited by Richard A. Flavell, Yale University School of Medicine, New Haven, CT, and approved July 29, 2004 (received for review February 26, 2004)

Neuronal death is often preceded by functional alterations at nerve terminals. Anti- and proapoptotic BCL-2 family proteins not only regulate the neuronal death pathway but also affect excitability of healthy neurons. We found that exposure of squid stellate ganglia to hypoxia, a death stimulus for neurons, causes a cysteine protease-dependent loss of full-length antiapoptotic BCL-xL, similar to previous findings in mammalian cells. Therefore, to determine the direct effect of the naturally occurring proapoptotic cleavage product of BCL-xL on mitochondria, recombinant N-truncated BCL-xL was applied to mitochondria inside the squid presynaptic terminal and to purified mitochondria isolated from yeast. N-truncated BCL-xL rapidly induced large multi-conductance channels with a maximal conductance significantly larger than those produced by full-length BCL-xL. This activity required the hydrophobic C terminus and the BH3 domain of BCL-xL. Moreover, N-truncated BCL-xL failed to produce any channel activity when applied to plasma membranes, suggesting that a component of the mitochondrial membrane is necessary for its actions. Consistent with this idea, the large channels induced by N-truncated BCL-xL are inhibited by NADH and require the presence of VDAC, a voltage-dependent anion channel present in the outer mitochondrial membrane. These observations suggest that the mitochondrial channels specific to full-length and N-truncated BCL-xL contribute to their opposite effects on synaptic transmission, and are consistent with their opposite effects on the cell death pathway.

BCL-xL is a potent inhibitor of programmed cell death and is abundantly expressed in neurons of the adult brain (1–5). BCL-xL localizes to the outer mitochondrial membrane (6) and has been suggested to protect cells from death by regulating export of ATP from mitochondria and/or by blocking the activation of proapoptotic BCL-2-related proteins (7–9). Under certain conditions, however, the antiapoptotic proteins BCL-xL and BCL-2 can be converted into BAX-like killer proteins by proteolytic cleavage of their N-terminal loop domain (10–13). Activation of proapoptotic molecules such as BAX causes the release of pro-death factors stored in the intermembrane space (14–17). Proapoptotic BCL-2 family proteins induce pores in purified mitochondrial outer membrane preparations and can release large molecules from pure liposomes (18–20).

Whether the proapoptotic BCL-2 family proteins induce the formation of pores in the outer mitochondrial membrane *in vivo*, and, if so, whether this channel formation requires specific interactions with mitochondrial membrane components is not yet known. A variety of lines of evidence suggest that BCL-2 family proteins may interact, either directly or indirectly, with the voltage-dependent anion channels VDAC-1 and VDAC-2, components of the outer mitochondrial membrane (21–23).

We have shown previously that BCL-xL immunoreactivity is present in presynaptic terminals of the giant synapse of squid stellate ganglia (24), where it is colocalized with mitochondria. When applied in a patch pipette to intact mitochondria within the terminal, full-length BCL-xL forms channels (≈200–500 pS) in the outer mitochondrial membrane. It also enhances synaptic transmission when injected directly into the presynaptic terminal.

During programmed cell death, proteases can cleave and enhance/activate the pro-death function of several BCL-2 family proteins including BID, BAD, BCL-2, BAX and BCL-xL (10, 11, 25–29). Although proteases are apparently not essential for activation of BAX, cleavage of BID by caspases may be required to promote cell death (27, 28). The antiapoptotic BCL-xL protein can be cleaved between the BH4 and BH3 domains by benzyloxycarbonyl-Val-Ala-Asp (zVAD)-sensitive proteases caspase-3 (Asp-61, Asp-76) and calpain (Ala-60) to produce a potently proapoptotic C-terminal fragment, ΔN BCL-xL (11, 12, 30). In mammalian cells, overexpression of ΔN BCL-xL (lacking amino acids 2–76) induces loss of mitochondrial membrane potential, cytochrome *c* release from mitochondria, and apoptosis (13, 26). In contrast to full-length BCL-xL, when injected into the presynaptic terminal of the squid giant synapse, ΔN BCL-xL attenuates synaptic transmission (24).

In this study, we demonstrate that application of ΔN BCL-xL to mitochondrial membranes in intact nerve terminals produces large multiconductance channel activity. This activity depends on an intact BH3 domain and on interaction with the mitochondrial membrane. The channel activity produced by ΔN BCL-xL is attenuated by NADH, an inhibitor of VDAC. Moreover, ΔN BCL-xL fails to induce NADH-sensitive channels in yeast mitochondria lacking VDAC-1. Our findings indicate that BCL-xL is cleaved under hypoxic conditions and suggest that the apoptotic cleavage fragment ΔN BCL-xL induces large-multiconductance channel activity in the outer mitochondrial membrane. The newly formed channels may flux ions, promote export of cytochrome *c*, or modulate other functions of mitochondria.

Methods

Intracellular Membrane Patch Clamp Recordings. Experiments were performed on small *Loligo pealei*. Bathing solution (466 mM NaCl/54 mM $MgCl_2$/11 mM $CaCl_2$/10 mM KCl/3 mM

This paper was submitted directly (Track II) to the PNAS office.

Abbreviations: VDAC, voltage-dependent anion channel; zVAD, benzyloxycarbonyl-Val-Ala-Asp; ANTS, 8-aminonapthalene-1,3,6–trisulfonic acid.

††To whom correspondence may be addressed. E-mail: hardwick@jhu.edu or leonard.kaczmarek@yale.edu.

$NaHCO_3$/10 mM Hepes, pH 7.2) was cooled, oxygenated with 99.5% O_2, 0.5% CO_2, and perfused over isolated stellate ganglia. Intracellular membrane pipettes (20–80 MΩ) were filled with intracellular solution which contained 570 mM KCl, 1.2 mM $MgCl_2$, 10 mM Hepes, 0.07 mM EGTA, 0.046 mM $CaCl_2$, and 2 mM ATP (pH 7.2). The intracellular membrane patch pipette was placed in an outer pipette that was inserted into the presynaptic terminal ≈50–100 μm from its distal end, during monitoring of membrane potential (24, 31, 32). The outer microelectrode was then retracted, exposing the inner tip to form a gigaohm seal. The polarities of potentials reported refer to those of the patch pipette relative to that of the ground electrode. Because of the difficulty of patch clamping plasma membranes in squid ganglia, isolated bag cell neurons of the mollusk *Aplysia californica* were used for plasma membrane experiments. Pipettes were either the same as those used for intracellular patch clamping or more conventional larger pipettes. Sample rate was 20 kHz, and data were filtered at 500-1000 Hz.

Protein Purification. BCL-xL and mutants were all produced as GST fusion proteins in *Escherichia coli*, by using a pGEX system (Pharmacia Biotech). Fusion proteins were induced with 0.1 mM isopropyl β-D-thiogalactoside (IPTG) for 6 h at 37°C and purified by affinity chromatography, by using glutathione-Sepharose 4B. BCL-xL proteins were cleaved from GST by thrombin, equilibrated in PBS (150 mM NaCl, 20 mM Na_2PO_4, pH 7.2), and stored at −80°C. All recombinant proteins were added to the intracellular patch solution at a concentration of 8 μg/ml. The C-terminal truncation of BCL-xL is lacking the last 21 aa.

Production of Liposomes. For measurements of ΔN BCL-xL-induced leakage from liposomes, dry lipid films were resuspended in the fluorophore 8-aminonapthalene-1,3,6–trisulfonic acid (ANTS, 12.5 mM) and its quencher, *p*-xylene-bis-piridinium bromide (DPX, 45 mM) in 10 mM Hepes, 0.2 mM EDTA (pH 7.0), and subjected to 10 freeze-thaw cycles, followed by extrusion through two polycarbonate membranes (0.1-μm pore). Lipid vesicles were separated from unencapsulated materials on Sephadex G-10 by using 100 mM KCl, 10 mM Hepes, 0.2 mM EDTA (pH 7.0) as elution buffer. The leakage of ANTS was monitored in a spectrometer with a thermostated 1-cm path length cuvette with constant stirring at 37°C. ANTS release was quantified on a percentage basis according to the equation: % leakage $= [(F_f - F_0)/(F_{100} - F_0)] \times 100$, F_f being the equilibrium value of fluorescence after protein addition, F_0 the initial fluorescence of the intact vesicle suspension, and F_{100} the fluorescence value after complete disruption of vesicle integrity by Tx-100 addition (0.2% wt/vol).

Immunoblots. Isolation of mitochondria from squid stellate ganglia was adapted from previous protocols (33, 34). Ganglia (16–20) were placed in unoxygenated seawater with zVAD-fluoromethyl ketone (zVAD-fmk) (100 μM) or DMSO vehicle control for 20 min, minced in ice-cold isolation buffer (500 mM mannitol/150 mM KCl/2 mM sodium-EDTA/1% fatty acid-free BSA/25 mM Hepes, adjusted to pH 7.4 with HCl at 25°C), homogenized with 12 strokes of a 2-ml Dounce homogenizer and centrifuged at 2,800 × *g* for 3 min at 4°C. The supernatant was centrifuged at 15,000 × *g* for 10 min at 4°C, washed, and recentrifuged. Mitochondria were stored frozen at −20°C. On thawing, 1 μl of general use protease inhibitor mixture was added. For detection of BCL-xL, 150 μg of squid mitochondrial protein and 4 ng of recombinant human BCL-xL, or 800 μg of whole cell lysates were separated on a 13% SDS gel and immunoblotted with anti-chicken BCL-xL rabbit polyclonal antibody provided by C. Thompson (University of Pennsylvania, Philadelphia) (1:1,000 dilution). For the preadsorption control, the antibody was preincubated with 0.2 μg/ml of recombinant human BCL-xL for 1 h at 22°C before incubation with the membrane. VDAC-1 was detected on the same membrane as a loading control by using a 1:500 dilution of N-18 goat polyclonal primary antibody.

To prepare hypoxic tissues for immunoblotting, ganglia were placed in a sealed filled tube of artificial seawater for 20–60 min before homogenization. Measurements of oxygen levels with an oxygen electrode (Hansatech Instruments, Pentney King's Lynn, U.K.) indicate that oxygen content of the medium under these conditions fell by 48.1 ± 1.1% ($n = 3$) from 320 to 166 nmol/ml.

Yeast Mitochondrial Recordings. Mitochondria were isolated from *Saccharomyces cerevisiae* grown in lactose media and harvested in log phase as described (35–37). Wild type (strain M3) and a strain of yeast, M22-2 (por1) in which por1 (YVDAC1) had been deleted (38), were used as indicated. Homogenization buffer was 0.6 M sorbitol, 10 mM Tris, 1 mM EDTA, 0.2% BSA, and 1 mM PMSF (pH 7.4) containing protease inhibitor mixture (Sigma, P 8215). Cell walls were weakened by lyticase treatment before homogenization. Isolated mitochondria were rapidly frozen in liquid nitrogen and stored at −80°C in 230 mM mannitol, 70 mM sucrose, 1 mM EDTA, and 5 mM Hepes (pH 7.4). For patch clamp recordings, the cells were placed in 150 mM KCl and 20 mM Hepes (pH 7.2), and the internal patch solution was of the same composition.

Results

Proapoptotic ΔN BCL-xL Induces Multiconductance Channels. As described (24, 32), mitochondria are the predominant organelles inside the squid presynaptic terminal and are the only organelles compatible in size with seal formation by patch pipettes. Purified recombinant BCL-xL proteins were placed inside the patch pipette used to record from mitochondria inside the squid nerve terminal. The recombinant N-truncated fragment of BCL-xL, ΔN BCL-xL, was shown previously to form large pores in lipid membranes and to induce cytochrome *c* release from isolated mitochondria (7), consistent with its proapoptotic function in mammalian cells (11, 26), When added directly to endogenous mitochondria, ΔN BCL-xL induced large channels (>760 pS) with multiple levels of conductance (Fig. 1*a*). ΔN BCL-xL induced large channels (>760 pS) with multiple levels of conductance (Fig. 1*a*). Consistent with previous reports, control recordings with no protein or application of full-length BCL-xL produced channel activity of lower conductance (24, 32) (Fig. 1*c*). The current–voltage relations for the ΔN BCL-xL-induced channels were measured by rapidly stepping the holding potential across a range of voltages during a series of openings at one conductance level. Current–voltage relations for the channel induced by ΔN BCL-xL were approximately linear, with a reversal potential close to 0 mV (Fig. 1*b*). The large conductance activity, with unitary openings corresponding to conductances between 300 pS and 3.8 nS, could usually be detected within one minute after seal formation. The maximal unitary current with ΔN BCL-xL in the pipette was significantly greater than in control recordings ($P < 0.0009$, $n = 6$).

To analyze further the effects of ΔN BCL-xL, and to compare different experiments, channel openings were divided into three groups according to their conductance. Small openings were defined as those with conductances <180 pS, and these comprise the majority of openings in control recordings (24, 32). Because previous work has shown that full-length BCL-xL induces channels with conductances <760 pS (24), intermediate conductances were defined as those between 180 pS and 760 pS. Large conductances were defined as >760 pS. Openings were assigned to these groups on the basis of peaks in amplitude histograms of channel activity. Bar graphs of the frequency of occurrence of different conductance levels demonstrate that large conduc-

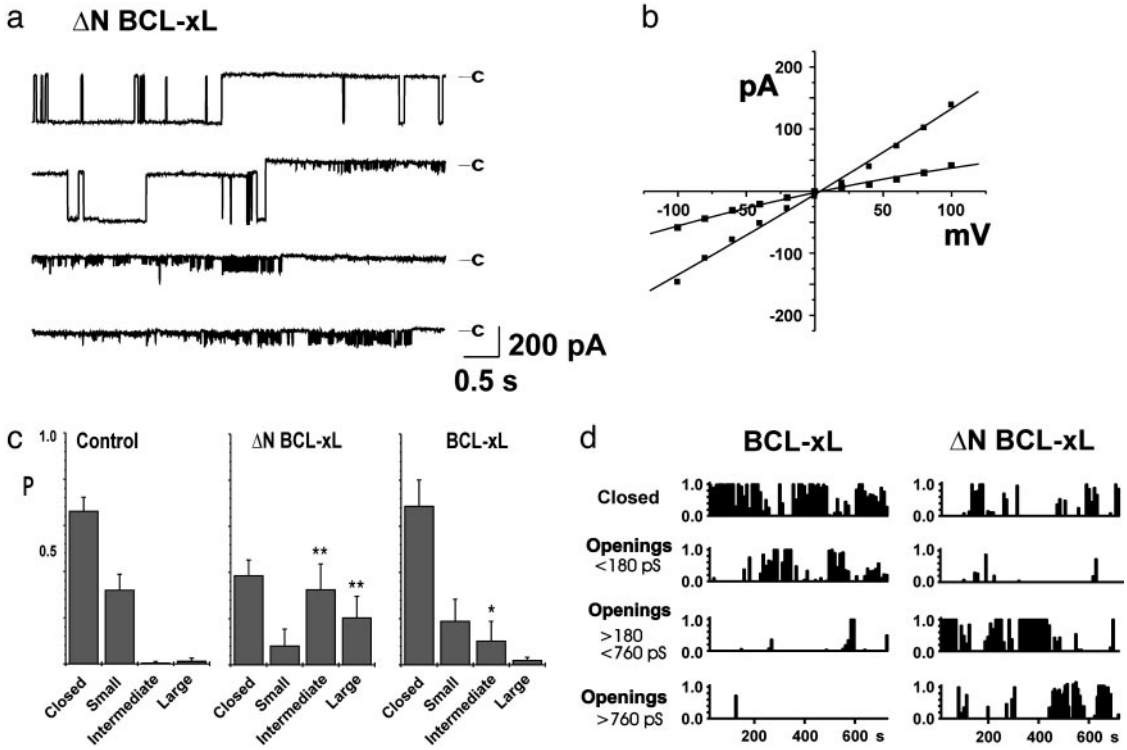

Fig. 1. Mitochondrial channel activity produced by ΔN BCL-xL. (*a*) Channel activity recorded at −100 mV using pipettes containing 8.0 μg/ml ΔN BCL-xL. (*b*) I-V relations for ΔN BCL-xL-induced activity, showing examples of intermediate and large conductances. (*c*) Cumulative distribution of probability of channel activity of different conductances in experiments with control intracellular solution, ΔN BCL-xL, or full-length BCL-xL. Histograms combining all experiments show the probability of closed channels, activity <180 pS (Small), activity between 180 and 760 pS (Intermediate), and activity >760 pS (Large). For controls, $n = 16$; for ΔN BCL-xL, $n = 6$; for FL BCL-xL, $n = 4$ (probabilities relative to control *, $P < 0.025$; **, $P < 0.005$). (*d*) Time course of transitions of channel opening to different conductances. Shown are transitions in recordings with 8.0 μg/ml ΔN BCL-xL (*Right*) or full-length BCL-xL (*Left*) in the patch pipette solution. Openings were divided into the three groups as above. Probability of occurrence of openings in each group within successive 10-s recording periods is plotted as a function of time.

tances occur with much greater frequency in patches containing ΔN BCL-xL than in controls or in those with full-length BCL-xL (Fig. 1*c*).

Channel activity produced by ΔN BCL-xL underwent reversible transitions between intermediate and large conductance levels and also frequently gated repeatedly to a single amplitude level for periods of time up to tens of seconds. This result is illustrated in Fig. 1*d*, which represents over 10 min of recording divided into 10-s blocks. The proportion of time spent at these conductance levels was determined for ΔN BCL-xL and for full-length BCL-xL. In contrast to full-length BCL-xL, the majority of the openings with ΔN BCL-xL were large (Figs. 1*d*).

To explore the specificity of ΔN BCL-xL for the induction of channel activity, a BH3 deletion mutant (lacking amino acids 90–92) was placed in the patch pipette. BH3 domains are conserved in both anti- and proapoptotic BCL-2 family proteins and have been suggested to promote cell death by binding into the cleft of partner BCL-2 proteins (39–41). Although this ΔN/Δ90-92-BCL-xL mutant retains the putative BH1-BH2 pore-forming region, it fails to kill transfected cells (11) and failed to produce any intermediate or large conductance ion channel activity in mitochondrial patches ($n = 4$, Fig. 2*b*). Similarly, deletion of the C-terminal hydrophobic membrane-anchor domain (ΔC20) that targets BCL-xL to mitochondrial membranes also abolished the ability of ΔN BCL-xL to produce channel activity different from control recordings when added to the patch pipette ($n = 2$, data at shown). Thus, the induction of channel activity by ΔN BCL-xL correlates with its ability to kill cells and to associate with mitochondria.

To determine whether ΔN BCL-xL can induce channel activity on other biological membranes, we tested its effects on the plasma membrane of molluscan neurons. In contrast to its effects on mitochondrial membranes, ΔN BCL-xL failed to induce any activity in plasma membranes ($n = 11$, Fig. 2*c*). In all such recordings, the normal pattern of endogenous small conductance (<100 pS) plasma membrane channel activity was detected (42) and did not seem to be influenced by the presence of ΔN BCL-xL. This finding suggests that a component of mitochondrial membranes is required for ΔN BCL-xL to produce its characteristic channel activity or that some property of the

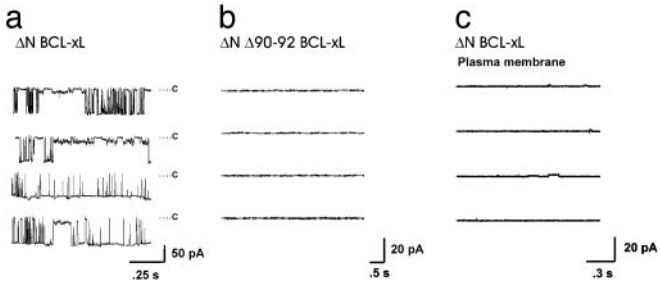

Fig. 2. Specificity of channel formation by ΔN BCL-xL. (*a*) Activity on a mitochondrial membrane recorded at −100 mV using a pipette containing 8.0 μg/ml ΔN BCL-xL. C marks the closed state. (*b*) Lack of activity in the presence of the BH3 domain mutant ΔN Δ90-92 BCL-xL. Patch potential was −100 mV. (*c*) Lack of effect of ΔN BCL-xL in cell-attached plasma membrane recordings of molluscan neurons. Endogenous small-conductance plasma membrane channel activity (42) can be detected. Patch potential was −160 mV.

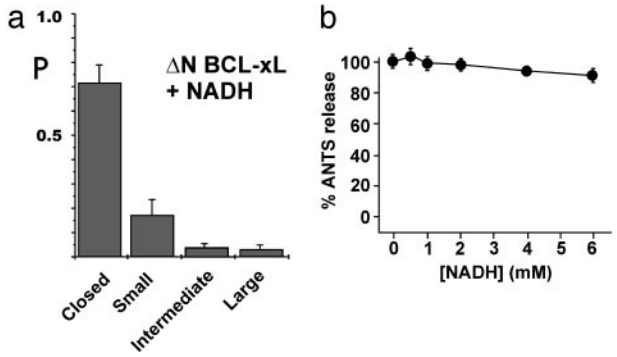

Fig. 3. Effects of NADH on multiconductance channel activity produced by ΔN BCL-xL. (*a*) Bar graphs show distribution of openings for patches exposed to 8.0 μg/ml ΔN BCL-xL with 2 mM NADH ($n = 10$). (*b*) Lack of effect of NADH on the release of fluorescent indicator (ANTS) from artificial lipid vesicles in the presence of ΔN BCL-xL. Lipid and protein concentrations were 50 μM and 50 nM, respectively.

plasma membrane inhibits the formation of channels by ΔN BCL-xL.

Channels Induced by ΔN BCL-xL Are Attenuated by NADH. Because the gigaohm seals were formed directly on intracellular organelles within the presynaptic terminal, it is likely that the membrane contacted by the patch pipette is the outer mitochondrial membrane. The conductance of this membrane is known to be reduced by millimolar concentrations of NADH (43, 44). A potential target of NADH is VDAC, a relatively nonselective channel that is believed to be the major conductance pathway across the outer membrane. This idea is based in part on the observation that NADH reduces the conductance of purified VDAC in lipid bilayers (43, 44). To determine the effect of NADH on ΔN BCL-xL, NADH was added to the intracellular patch pipette. The probability of large conductance activity induced by ΔN BCL-xL in mitochondrial membranes was significantly reduced by NADH ($n = 10$, Fig. 3*a*). NADH did not prevent the insertion of ΔN BCL-xL into mitochondrial membranes, because channel activity could sometimes be detected transiently after seal formation (data not shown).

NADH Fails to Block ΔN BCL-xL Conductance in Lipid Vesicles. ΔN BCL-xL has been shown to induce pore formation in synthetic lipid vesicles (7, 13). Therefore, to determine whether NADH works directly on ΔN BCL-xL, we also tested NADH on the action of ΔN BCL-xL in synthetic lipid vesicles with no other mitochondrial components present. In contrast to the inhibitory effects of NADH on ΔN BCL-xL-induced channels on mitochondria in living cells, NADH did not antagonize the effects of ΔN BCL-xL on the permeability of artificial lipid membranes, which was determined by measuring the leakage of the fluorophore ANTS from liposomes (Fig. 3*b*). Konig's polyanion, another blocker of mitochondrial conductances (44), was found to be nonspecific, in that it inhibited all mitochondrial channel activity and also blocked the action of ΔN BCL-xL in lipid membranes (data not shown). Taken together, the data suggest that NADH alters the conductance of ΔN BCL-xL-induced channels by acting on a mitochondrial component other than the BCL-xL protein.

Formation of NADH-Sensitive Channels by ΔN BCL-xL Requires VDAC. To investigate the hypothesis that the channel induced by ΔN BCL-xL results from an interaction with VDAC, we tested the actions of ΔN BCL-xL on isolated mitochondria prepared from

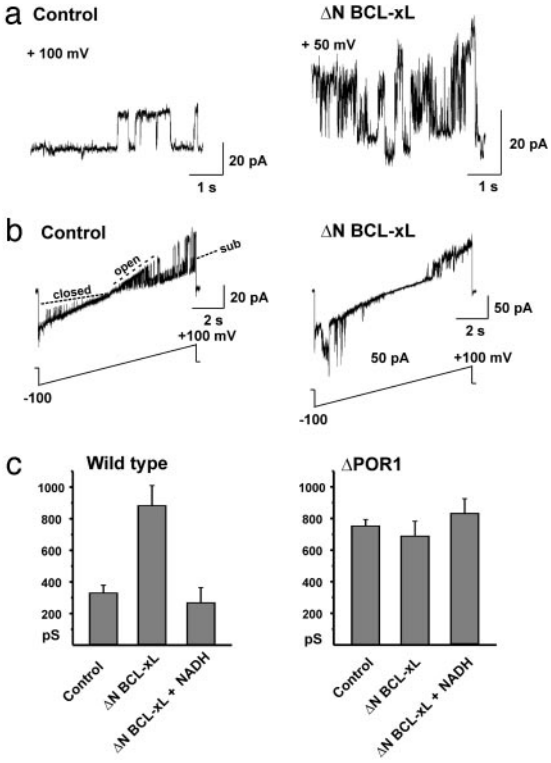

Fig. 4. Actions of ΔN BCL-xL on channel activity in isolated mitochondria from wild-type yeast and those lacking the POR1 gene (ΔPOR1). (*a*) Typical channel activity in wild-type yeast mitochondria in the absence (*Left*) or presence (*Right*) of 8.0 μg/ml ΔN BCL-xL. (*b*) Channel activity during a 10-s ramp from −100 to +100 mV. Holding potential before and after the ramp was 0 mV. (*Left*) Response in the absence of ΔN BCL-xL. As expected for the VDAC, increased channel openings occur near the center of the ramp. The slope of the closed state is indicated, as is the slope of the subconductance state (sub) that persists at positive and negative potentials. (*Right*) Response with 8.0 μg/ml ΔN BCL-xL. (*c*) Bar graphs show the maximal channel conductance recorded in the absence or presence of 8.0 μg/ml ΔN BCL-xL, or of ΔN BCL-xL with 2 mM NADH. Shown are data for wild-type mitochondria (*Left*) and ΔPOR1 mutant mitochondria (*Right*).

wild-type yeast and from yeast that lack the *por1* gene, which encodes the VDAC-1 channel (YVDAC1) (45, 46).

Recording from the outer membrane of isolated wild-type yeast mitochondria, we detected voltage-dependent behavior with properties similar to that previously described for VDAC in artificial membranes (47) (Fig. 4*a*). Specifically, repeated gating to an open state could be detected in the voltage range −10 to +40 mV, but at more positive or negative potentials the channel was more likely to close to a lower subconductance state (Fig. 4*b*). Even at these polarized potentials, however, multiconductance activity could be detected. The dominant conductance in all such recordings from wild-type mitochondria was between 200 and 400 pS (mean = 325 ± 48 pS, $n = 9$). In a separate set of recordings, the inclusion of ΔN BCL-xL protein in the pipette solution resulted in a very different pattern of activity. The typical VDAC-like activity could no longer be detected, and significantly larger conductance activity was detected at both positive and negative potentials (Fig. 4 *a* and *b*). In the presence of ΔN BCL-xL, the dominant conductance of channel activity was between 500 pS and 1 nS (mean = 867 ± 79 pS, $n = 16$, $P < 0.0001$). (As appropriate for yeast, recordings were made with external and pipette media of lower ionic strength than for squid mitochondria.) These large conductances were markedly attenuated by the addition of NADH to the pipette and bath solutions (Fig. 4*c*, $n = 9$, $P < 0.0015$).

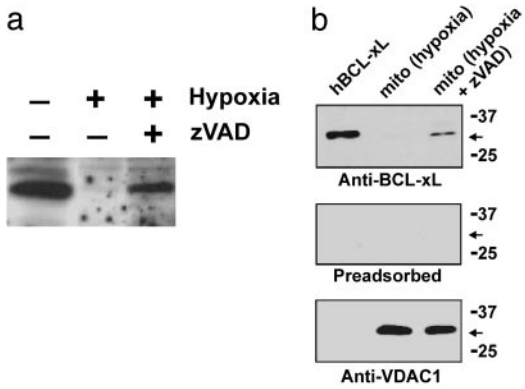

Fig. 5. zVAD prevents loss of full-length BCL-xL protein during hypoxia. (*a*) Immunoblot of untreated or hypoxia-treated (60 min) squid stellate ganglia incubated in the absence or presence of zVAD (100 μM) by using anti-chicken BCL-x antibody. Equal loading was verified by comparing a crossreacting band near the top of the gel. (*b*) Immunoblot of recombinant human BCL-xL protein and of mitochondria (mito) purified from hypoxic (20 min) squid stellate ganglia ($\pm$ zVAD) by using anti-Bcl-x antibody (*Top*). (*Middle*) Immunoblots using the same antibody preadsorbed with recombinant human BCL-xL protein. (*Bottom*) Immunoblot analysis using an anti-VDAC antibody.

Large conductance activity could be recorded under control conditions in mitochondrial membranes from mutant ΔPOR1 yeast lacking the VDAC. This activity was significantly greater than that in wild-type mitochondria ($n = 8$, $P < 0.001$). In contrast to the wild-type mitochondria, however, this activity was completely unaffected by ΔN BCL-xL and was not inhibited by NADH ($n = 7$, Fig. 4*c*), suggesting that the large conductances detected in the ΔPOR1 mitochondria are pharmacologically unrelated to those induced by ΔN BCL-xL in the wild-type VDAC-containing mitochondria.

zVAD Inhibits Proteolysis of BCL-xL During Hypoxia. We hypothesize that ΔN BCL-xL or related proapoptotic molecules could be formed rapidly in response to a death stimulus. Because the pro-death function of many BCL-2 family proteins, like BCL-xL, may be activated by proteolysis, we tested whether proteolysis of BCL-xL occurs endogenously in response to a death stimulus. Squid stellate ganglia were exposed to hypoxia for 20 min, in the presence or absence of zVAD, a pan caspase/calpain inhibitor that inhibits cell death. The ganglia were then analyzed for BCL-xL protein. A BCL-xL immunoreactive band was detected in whole cell lysates prepared from freshly explanted ganglia and from hypoxic ganglia treated with zVAD. In contrast, this same band was nearly absent in hypoxic ganglia treated with DMSO carrier control (Fig. 5*a*). To confirm this result, mitochondria were purified from squid ganglia that had been incubated without oxygenation for 20 min in the presence of zVAD or DMSO carrier control. Immunoblot analysis of isolated squid mitochondria detected a BCL-xL immunoreactive band of the same size as recombinant human BCL-xL protein, and squid mitochondrial BCL-xL was significantly reduced in the absence of zVAD (Fig. 5*b Top*). Preincubating the antibody with recombinant human BCL-xL protein blocked immunodetection of both squid and human BCL-xL protein (Fig. 5*b Middle*). VDAC protein was present at similar levels in both the zVAD-treated and untreated squid mitochondrial preparations (Fig. 5*b Bottom*). This finding verifies equal loading of mitochondrial samples and demonstrates that protein degradation was not a general feature of the hypoxic sample. The only BCL-xL antibodies that cross react with squid do not recognize ΔN BCL-xL. Therefore, the disappearance of BCL-xL during hypoxia could be due to caspase-like proteolytic cleavage and/or to complete degradation after a zVAD-sensitive event.

Discussion

Previous work has indicated that protease activation and increased levels of pro-death BCL-2 family members occur during ischemic injury (48), and that rundown of neurotransmission is one of the earliest events in hypoxic injury to a neuron (49, 50). We have found that immunoreactive BCL-xL is present on mitochondria in the squid stellate ganglion and that, like hypoxia, injection of ΔN BCL-xL into the presynaptic terminal causes rundown of synaptic transmission (24). By recording intact mitochondria in a living nerve terminal, we have now found that ΔN BCL-xL induces large multiconductance channel activity that is significantly greater than that produced by full-length BCL-xL or that detected in control recordings. Major increases in the permeability of the outer mitochondrial membrane are usually associated with apoptosis. It is important to emphasize, however, that BCL-xL is present at high levels in mitochondria of adult neurons within synaptic terminals that are located very far from the neuronal somata where mitochondria are thought to control apoptosis. In the case of the squid giant synapse, the BCL-xL-containing synaptic mitochondria are located many centimeters from the somata. Thus, it is possible that, rather than determining cell fate, the regulation of mitochondrial permeability by BCL-xL at these distal sites plays a local role in regulating synaptic activity. For example, alterations in mitochondrial metabolism or the release of substances from the intermembrane space produced by these large conductance channels may contribute to the rundown of synaptic transmission produced by ΔN BCL-xL.

Four findings strongly suggest that the channel activity produced by ΔN BCL-xL results from its interaction with an endogenous mitochondrial factor. (*i*) ΔN BCL-xL failed to produce large conductance activity in plasma membranes. (*ii*) The ΔN BCL-xL-induced conductances in mitochondrial membranes could be antagonized by NADH, whereas this agent had no effect on the permeability of pure lipid membranes exposed to ΔN BCL-xL. (*iii*) The regular large-conductance openings produced by ΔN BCL-xL in mitochondria differ from the "lipidic pores" previously described in lipid bilayers exposed to ΔN BCL-xL, where irregular increases in membrane current rapidly produce collapse of the bilayer (13). (*iv*) The activity of ΔN BCL-xL differs from the small channels induced on intracellular mitochondria by full-length BCL-xL (24), although both have the same putative pore-forming domain between domains BH1 and BH2 (51).

By comparing VDAC-containing and VDAC-deficient mitochondria isolated from yeast, we found that VDAC is required for ΔN BCL-xL to produce NADH-sensitive channel activity. Although there are other possible explanations, our data are consistent with the hypothesis that ΔN BCL-xL interacts, directly or indirectly, with VDAC to alter the properties/function of VDAC in both yeast and synaptic mitochondria. The channel activity produced by ΔN BCL-xL in wild-type yeast mitochondria shares biophysical as well as pharmacological properties with that detected in the squid presynaptic terminal after application of ΔN BCL-xL. In particular, the ΔN BCL-xL-induced channel activity in yeast mitochondria is not voltage-dependent and has a large conductance of 500 pS to 1 nS. In the mitochondria lacking VDAC, although channel activity could be detected, these large channels differed pharmacologically from those in VDAC-containing mitochondria. Specifically, the large conductance activity found in the outer membrane of the POR1-deficient mitochondria was not inhibited by NADH, suggesting that, as found previously in permeation studies (46), NADH fails to interact with the outer membrane channels in POR1-deficient mitochondria.

Our results also show that proteolysis of endogenous BCL-xL occurs in the squid ganglion in response to hypoxia. Mammalian caspases and other factors have been found to play a role in cell death both before and after the release of cytochrome *c* and other protease-activating factors from mitochondria (10, 13, 26). Although we were not able to identify any of the cleavage products of BCL-xL in squid, and cannot therefore be certain that an endogenous ΔN BCL-xL-like protein is formed, it is likely that, as in mammalian systems, proapoptotic fragments of BCL-xL are generated by the actions of caspases or other proteases.

BCL-2 family proteins may regulate apoptosis but their effect on the permeability of the outer mitochondrial membrane may also control physiological processes unrelated to acute cell death (20, 24, 52). Because previous work has shown that certain forms of synaptic plasticity are associated with changes in mitochondrial membrane conductances (32), it is possible that proteins previously implicated in apoptosis may also regulate plastic changes in the mature nervous system (24, 52).

We thank Michael Forte (Vollum Institute, Portland, OR) for the yeast strains and Zane Andrews for the oxygen measurements. This work was supported by National Institutes of Health Grants NS18496 (to L.K.K.), NS37402 and NS34175 (to J.M.H.), GM57249 (to K.W.K.), and NS45876 (to E.A.J.). E.A.J. is an Established Investigator of the American Heart Association.

1. Boise, L. H., González-Garcia, M., Postema, C. E., Ding, L., Lindstein, T., Turka, L. A., Mao, X., Nûñez, G. & Thompson, C. B. (1993) *Cell* **74,** 597–608.
2. Krajewski, S., Krajewska, M., Shabaik, A., Wang, H. G., Irie, S., Fong, L. & Reed, J. C. (1994) *Cancer Res*. **54,** 5501–5507.
3. González-Garcia, M., Garcia, I., Ding, L., O'Shea, S., Boise, L. H., Thompson, C. B. & Nunez, G. (1995). (1995) *Proc. Natl. Acad. Sci. USA* **92,** 4304–4309.
4. Frankowski, H., Missotten, M., Fernandez, P. A., Martinou, I., Michel, P., Sadoul, R. & Martinou, J. C. (1995) *NeuroReport* **6,** 1917–1921.
5. Blömer, U., Kafri, T., Randolph-Moore, L., Verma, I. M. & Gage, F. H. (1998) *Proc. Natl. Acad. Sci. USA* **95,** 2603–2608.
6. Kaufmann, T., Schlipf, S., Sanz. J., Neubert, K., Stein, R. & Borner, C. (2003) *J. Cell Biol*. **160,** 53–64.
7. Basañez, G., Sharpe, J. C., Galanis, J., Brandt, T. A., Hardwick, J. M. & Zimmerberg, J. (2002) *J. Biol. Chem*. **277,** 49360–49365.
8. Vander Heiden, M. G., Chandel, N. S., Li, X. X., Schumacker, P. T., Colombini, M. & Thompson, C. B. (2000) *Proc. Natl. Acad. Sci. USA* **97,** 4666–4667.
9. Zong, W. X., Lindston, T., Ross, A. J., MacGregor, G. R. & Thompson, C. B. (2001) *Genes Dev*. **15,** 1481–1486.
10. Cheng, E. H. Y., Kirsch, D. G., Clem, R. J., Ravi, R., Kastan, M. B., Bedi, A., Ueno, K. & Hardwick, J. M. (1997) *Science* **278,** 1966–1968.
11. Clem, R. J., Cheng, E. H. Y., Karp, C. L., Kirsch, D. G., Ueno, K., Takahashi, A., Kastan, M. B., Griffin, D. E., Earnshaw, W. C., Veliuona, M. A. & Hardwick, J. M. (1998) *Proc. Natl. Acad. Sci*. USA **95,** 554–559.
12. Fujita, N., Nagahashi, A., Nagashima, K., Rokudai, S. & Tsuruo, T. (1998) *Oncogene* **17,** 1295–1304.
13. Basañez, G., Zhang, J., Chau, B. N., Maksaev, G. I., Frolov, V., Brandt, T. A., Burch, J., Hardwick, J. M. & Zimmerberg, J. (2001) *J. Biol. Chem*. **276,** 31083–31091.
14. Antonsson, B., Conti, F., Ciavatta, A., Montessuit, S., Lewis, S., Martinou, I., Bernasconi, L., Bernard, A., Mermod, J.-J., Mazzei, G., *et al*. (1997) *Science* **277,** 370–372.
15. Eskes, R., Antonsson, B., Osen-Sand, A., Montessuit, S., Richter, C., Sadoul, R., Mazzei, G., Nichols, A. & Martinou, J.-C. (1998) *J. Cell. Biol*. **143,** 217–224.
16. Martinou, J. C. & Green, D. R. (2001) *Nat. Rev. Mol. Cell. Biol*. **2,** 63–67.
17. Polster, B. M., Kinnally, K. W. & Fiskum, G. (2001) *J. Biol. Chem*. **276,** 37887–37894.
18. Basañez, G., Nechushtan, A., Drozhinin, O., Chanturiya, A., Choe, E., Tutt, S., Wood, K. A., Hsu, Y.-T., Zimmerberg, J. & Youle, R. J. (1999) *Proc. Natl. Acad. Sci. USA* **96,** 5492–5497.
19. Kuwana, T., Mackey, M. R., Perkins, G., Ellisman, M. H., Latterich, M., Schneiter, R., Green, D. R. & Newmeyer, D. D. (2002) *Cell* **111,** 331–342.
20. Pavlov, E. V., Priault, M., Pietkiewicz, D., Cheng, E. H. Y., Antonsson, B., Manon, S., Korsmeyer, S. J., Mannella, C. A. & Kinnally, K. W. (2001) *J. Cell. Biol*. **155,** 725–731.
21. Tsujimoto, U. & Shimizu, S. (2000) *Cell Death Differ*. **7,** 1174–1181.
22. Vander Heiden, M. G., Li, X. X., Gottleib, E., Hill, R. B., Thompson, C. B. & Colombini, M. (2001) *J. Biol. Chem*. **276,** 19414–19419.
23. Cheng, E. H., Sheiko, T. V., Fisher, J. K., Craigen, W. J. & Korsmeyer, S. J. (2003) *Science* **301,** 513–517.
24. Jonas, E. A, Hoit, D., Hickman, J. A., Zhang, J., Brandt, T. A., Yin, D., Ivanovska, I., Fannjiang, Y., McCarthy, E., Hardwick, J. M. & Kaczmarek, L. K. (2003) *J. Neurosci*. **23,** 8423–8431.
25. Condorelli, F., Salomoni, P., Cotteret, S., Cesi, V., Srinivasula, S. M., Elnemri, E. S. & Calabretta, B. (2001) *Mol. Cell. Biol*. **21,** 3025–3036.
26. Kirsch, D. G., Doseff, A., Chau, B. N., Lin, D.-S., de Souza-Pinto, N. C., Hansford, R., Kastan, M. B., Lazebnik, Y. A. & Hardwick, J. M. (1999) *J. Biol. Chem*. **274,** 21155–21161.
27. Li, H., Zhu, H., Xu, C. & Yuan, J. (1998) *Cell* **94,** 491–501.
28. Luo, X., Budihardjo, I., Zou, H., Slaughter, C. & Wang, X. (1998) *Cell* **94,** 481–490.
29. Wood, D. E. & Newcomb, E. W. (2000) *Exp. Cell Res*. **256,** 375–382.
30. Nakagawa, T. & Yuan, J. (2000) *J. Cell. Biol*. **150,** 887–894.
31. Jonas, E. A., Knox, R. J. & Kaczmarek, L. K. (1997) *Neuron* **19,** 7–13.
32. Jonas, E. A., Buchanan, J. & Kaczmarek, L. K. (1999) *Science* **286,** 1347–1350.
33. Mommsen, T. P. & Hochachka, P. W. (1981) *Eur. J. Biochem*. **120,** 345–352.
34. Rosenthal, R. E., Hamud, F., Fiskum, G., Varghese, P. J. & Sharpe, S. (1987) *Cereb. Blood Flow Metab*. **7,** 752–758.
35. Muro, C., Grigoriev, S. M., Pietkiewicz, D., Kinnally, K. W. & Campo, M. L. (2003) *Biophys. J*. **84,** 2981–2989.
36. Emtage, J. L. T. & Jensen R. E. (1993) *J. Cell Biol*. **122,** 1003–1012.
37. Daum, G., Böhni, P. & Schatz, G. (1982) *J. Biol. Chem*. **257,** 13028–13033.
38. Blachly-Dyson, E., Song, J., Wolfgang, W. J., Colombini, M. & Forte, M. (1997) *Mol. Cell. Biol*. **17,** 5727–5738.
39. Sattler, M., Liang, H., Nettesheim, D., Meadows, R. P., Harlan, J. E., Eberstadt, M., Yoon, H. S., Shuker, S. B., Chang, B. S., Minn, A. J., *et al*. (1997) *Science* **275,** 983–986.
40. Wang, K., Gross, A., Waksman, G. & Korsmeyer, S. J. (1998) *Mol. Cell. Biol*. **18,** 6083–6089.
41. Kelekar, A. & Thompson, C. B. (1998) *Trends Cell Biol*. **8,** 324–330.
42. Wilson, G. F., Magoski, N. S. & Kaczmarek, L. K. (1998) *Proc. Natl. Acad. Sci. USA* **95,** 10938–10943.
43. Lee, A. C., Zizi, M. & Colombini, M. (1994) *J. Biol. Chem*. **269,** 30974–30980.
44. Wunder, U. R. & Colombini, M. (1991) *J. Membr. Biol*. **123,** 83–91.
45. Lohret, T. A. & Kinnally, K. W. (1995) *Biophys. J*. **68,** 2299–2309.
46. Lee, A. C., Xu, X., Blachly-Dyson, E., Forte, M. & Colombini, M. (1998) *J. Membr. Biol*. **61,** 173–181.
47. Colombini, M., Blachly-Dyson, E. & Forte, M. (1996) *Ion Channels* **4,** 169–202.
48. Banasiak, K. J., Xia, Y. & Haddad, G. G. (2000) *Prog. Neurobiol*. **62,** 215–249.
49. Pang, Z. P., Deng, P., Ruan, Y. W. & Xu, Z. C. (2002) *J. Neurosci*. **22,** 10948–10957.
50. Tekkok, S. B., Godfraind, J. M. & Krnjevic, K. (2002) *Neuroscience* **113,** 11–21.
51. Muchmore, S. W., Sattler, M., Liang, H., Meadows, R. P., Harlan, J. E., Yoon, H. S., Nettesheim, D., Chang, B. S., Thompson, C. B., Wong, S. L., *et al*. (1996) *Nature* **381,** 335–341.
52. Fannjiang, Y., Kim, C. H., Huganir, R. L., Zou, S., Lindsten, T., Thompson, C. B., Mito, T., Traystman, R. J., Larsen, T., Griffin, D. E., *et al*. (2003) *Dev. Cell* **4,** 575–585.